Catalysis in Glycine *N*-Methyltransferase: Testing the Electrostatic Stabilization and Compression Hypothesis†

Alejandro Soriano,‡ Raquel Castillo, Christo Christov,§ Juan Andrés, and Vicente Moliner*

Departament de Ciències Experimentals, Universitat Jaume I, 12071 Castellón, Spain

Iñaki Tuñón*

Departament de Química Física, Universidad de Valencia, 46100 Burjasot, Valencia, Spain

Received June 30, 2006; Revised Manuscript Received September 20, 2006

ABSTRACT: Glycine *N*-methyltransferase (GNMT) is an *S*-adenosyl-L-methionine dependent enzyme that catalyzes glycine transformation to sarcosine. Here, we present a hybrid quantum mechanics/molecular mechanics (QM/MM) computational study of the reaction compared to the counterpart process in water. The process takes place through an S_N2 mechanism in both media with a transition state in which the transferring methyl group is placed in between the donor (SAM) and the acceptor (the amine group of glycine). Comparative analysis of structural, electrostatic, and electronic characteristics of the in-solution and enzymatic transition states allows us to get a deeper insight into the origins of the enzyme's catalytic power. We found that the enzyme is able to stabilize the substrate in its more active basic form by means of a positively charged residue (Arg175) placed in the active site. However, the maximum stabilization is attained for the transition state. In this case, the enzyme is able to form stronger hydrogen bonds with the positively charged amine group. Finally, we show that in agreement with previous computational studies on other methyltransferases, there is no computational evidence for the compression hypothesis, as was formulated by Schowen (Hegazi, M. F., Borchardt, R. T., and Schowen, R. L. (1979) *J. Am. Chem. Soc. 101*, 4359−4365).

Enzymes are able to speed up chemical reactions by several orders of magnitude, making metabolic transformations fast enough to be compatible with life (*1*). In fact, enzymes are amazing catalysts, not only because of their catalytic power but also because of their specificity and selectivity. The origin of this catalytic efficiency is still a controversial topic (*2*−*5*). In general, two different theories, with several variants, have been elaborated to explain enzymatic activity. The first, stresses the effect of the enzyme on the reaction transition state (TS[1]). According to TS theories, energy barrier reduction is attained by means of TS stabilization relative to the uncatalyzed process, the counterpart reaction in aqueous solution (*6*−*8*). This stabilization is mainly done by electrostatic interactions that take place in the enzyme but not in solution. The second theory explains the energy barrier reduction on the basis of a reactant state (RS) destabilization (*9*−*13*). An explanation based on the enhanced formation of an especially reactive conformation (near attack conformations or NACs) (*13*) in the enzyme can be interpreted as an example of these types of theories. Recently, some of us proposed that RS destabilization could be related to TS stabilization, considering that an active site complementary to the TS may favor the reactant conformation electronically and geometrically closer to the TS (*14*). Similarly, the work of García-Viloca et al. (*3*) shows and discusses that the two concepts are physically equivalent within the limits of transition state theory (TST) and amount only to two deceptively different descriptions of TS stabilization. The analysis of an increasing number of enzymatic systems is helpful to highlight this fundamental problem, although new challenges, such as the understanding of the coupling between reaction and protein dynamics (*15*, *16*), or the fact that TST may be inadequate to account for some catalytic effects (*2*), are emerging and requiring a more complex formulation.

† We are indebted to *DGI* for project BQU2003-04168, *BANCAIXA* for project P1-1B2002-02, P1-1B2005-13, and P1-1B2005-15, and *Generalitat Valenciana* for projects GV06-021, GV04B-131, GV06/152, GV06/016, ACOMP06/122, and GRUPOS04/08, which supported this research. A.S. is thankful for the Decom Valencia fellowship. The Marie Curie Development Host Fellowship program supported the work of C.C. (contract no. HPMD-CT-2000-00055). The authors are solely responsible for the information communicated, and it does not represent the opinion of The European Community. The European Community is not responsible for any use that might be made of data appearing herein. C.C. also acknowledges grant CTESIN/2004019 from *Generalitat Valenciana*, grant RIG 981486 from NATO, and grant YS-CH-1202 from the Bulgarian Science Fund.

* To whom correspondence should be addressed. Tel: 34-964-728-084. Fax: 34-964-728-066. E-mail: moliner@uji.es (V.M.); Tel: 34-963-544-880. Fax: 34-963-544-564. E-mail: tunon@uv.es (I.T.).

‡ Current address: Servei de Informática, Universidad de Valencia.

§ Current address: School of Chemistry, University of Bristol. On leave from Institute of Organic Chemistry, Bulgarian Academy of Sciences, 1113 Sofia, Bulgaria.

[1] Abbreviations: GNMT, glycine *N*-methyl transferase; QM/MM, quantum mechanics/molecular mechanics; SAM, *S*-adenosyl-methionine; SAH, *S*-adenosyl-L-homocysteine; TS, transition state; RS, reactant state; TST, transition state theory; PMF, potential of mean force; WHAM, weighted hystogram analysis method; ZW, zwitterionic form of glycine; BA, basic form of glycine; NE, neutral form of glycine; AC, acid form of glycine; KIE, kinetic isotope effect.

10.1021/bi061319k CCC: $33.50
Published on Web 11/23/2006

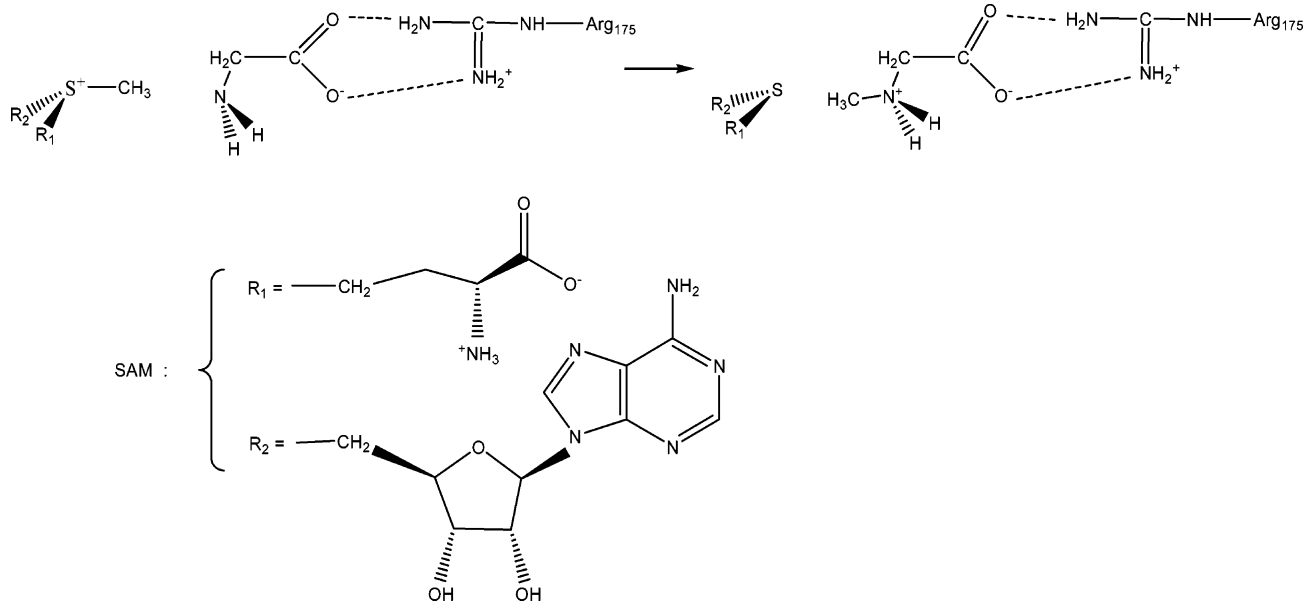

FIGURE 1: Schematic representation of SAM dependent methylation of glycine to form sarcosine.

Enzymes that catalyze transmethylation reactions using *S*-adenosyl-L-methionine (SAM) as the methyl donor appear in a variety of cellular processes involving nucleic acids, proteins, phospholipids, and some small molecules (*17*). Glycine *N*-methyltransferase (GNMT) catalyzes the SAM dependent methylation of glycine to form sarcosine (Figure 1) (*18*). GNMT is abundant in the liver, and the product sarcosine has no known physiological role and is converted back to glycine by sarcosine dehydrogenase (*19*). Unlike most SAM dependent methyltransferases this enzyme is weakly inhibited by its product *S*-adenosyl-L-homocysteine (SAH) (*20*), and then, it has been suggested that the role of the GNMT is to regulate the SAM/SAH ratio (*20*), which is important for other SAM dependent methyltranferases present in the cell. Crystal structures of GNMT complexed with SAM and acetate, a competitive inhibitor of glycine, and the R175K mutated enzyme complexed with SAM were determined at 2.8 and 3.0 Å resolutions, respectively (*21*). With these crystal structures and the previously determined structures of the substrate-free enzyme, a catalytic mechanism has been proposed by Konishi and Fujioka (*22*). According to this, GNMT binds its substrates in an obligatory order, with SAM as the first substrate. Structural changes occur in the transitions from the substrate-free to the binary complex and from the binary to the ternary complex. In the ternary complex stage, an α-helix in the *N*-terminus undergoes a major conformational change. As a result, SAM is firmly connected to the protein, and a glycine pocket is created near the bound SAM. The second substrate glycine binds to Arg175 and is brought into the glycine pocket. In the proposed structure, five hydrogen bonds connect the glycine in the proximity of the SAM and orient the lone pair orbital on the amino nitrogen (N) of glycine toward the donor methyl group (C) of SAM, preparing the subsequent S_N2 methyl transfer reaction. The mutagenesis studies also support the presented mechanism (*21*). The experimental k_{cat} of the wild-type enzyme measured at pH = 7.2 and 303 K is 27 min^{-1} (*21*).

Despite the interest shown from the experimental point of view, only one theoretical study about this enzyme has been published (*23*). In this article, the authors used density functional theory to study the methylation of glycine by SAM in a reduced gas phase model. The potential energy barrier calculated in this manner was found to be 15.0 kcal/mol, using the largest model formed by SAM and glycine plus Tyr21, Gly137, Asn138, and Tyr194. The position of some key atoms was kept frozen at their X-ray values in order to simulate the constraint imposed by the protein structure. S−EnDashC and C−N bond distances in the transition structure were calculated to be 2.28 and 2.18 Å, respectively. Some trials were also performed on the protonation state of the glycine. The authors studied how the protonation of the carboxyl group of the glycine affects the energy barrier. They found that the reaction takes place with a lower energy barrier when the glycine is in the negative form. Although useful conclusions can be obtained from this kind of calculations, it must be taken into account that there are drawbacks such as the lack of protein flexibility and long-range effects.

Here, we present a QM/MM study of the methyl transfer reaction catalyzed by GNMT. This methodology allows the study of the enzymatic reaction, taking into account the effect of the whole protein and solvent water molecules in a dynamic way by means of a flexible molecular model coupled to molecular dynamics (MD) simulations. The results are compared to the reaction in aqueous solution, allowing a deeper insight into the origin of enzyme catalysis. In particular, we analyze structural, electrostatic, and electronic features of the transition states in both media to understand the reason for barrier lowering in the enzyme.

MATERIALS AND METHODS

Building the Systems. To study the GNMT catalyzed reaction and its counterpart process in aqueous solution, we have used the QM/MM methodology (*24*−*27*) by means of the DYNAMO program (*28*). In this methodology, the total system is divided into two subsystems, and each is treated at a different level of theory. The SAM molecule and the glycine are chosen to be the QM subsystem, whereas the rest of the enzyme and/or water molecules are in the MM subsystem. There is no need for a special treatment for the

boundary between the QM and MM subsystems because there are no covalent bonds between the substrate or the cofactor and the enzyme. We have used the semiempirical Hamiltonian AM1 (*29*) to describe the QM subsystem. The MM subsystem was treated using the OPLS-AA force field (*30*) for the enzyme atoms, whereas the TIP3P potential (*31*) was used for the water molecules. All Lennard-Jones parameters for the QM subsystem are also taken from the OPLS-AA force field. A switched cutoff radius of 12 Å was used all around the simulations for all kinds of interactions.

For studying the enzyme reaction, the atomic coordinates were taken from the X-ray crystal structure with Protein Data Bank code 1NBH (*21*). This structure contains SAM and acetate as an inhibitor that was replaced by a glycine molecule overlapping the common parts of their structures. Then, we added the hydrogen atoms, and their positions were subsequently relaxed by means of a conjugate-gradient procedure. Afterward, the enzymatic system (enzyme plus SAM plus substrate) was placed in a cavity deleted from a 79.5 Å side box of TIP3P water molecules. The resulting system had 50 223 atoms. Water molecules were relaxed by means of a 40 ps NVT molecular dynamics (MD) simulation using a time step of 1 fs and a reference temperature of 300 K. All atoms beyond 25 Å of any atom of the SAM or glycine molecule were frozen (43 199 atoms in total) for any subsequent simulation. To study the reaction in aqueous solution, SAM and glycine were placed in the center of a 79.5 Å side box of water molecules, removing those overlapping the reactant molecules. As explained below, we tested two possible protonation states of glycine to analyze the reaction in water. The final number of water molecules was 16 801 for both aqueous solution models. Water molecules were relaxed following a procedure similar to that explained for the enzyme. In aqueous solution, periodic boundary conditions were used during all of the simulations.

Potential of Mean Force (PMF) Evaluation. PMFs in aqueous solution and in GNMT were computed using umbrella sampling methodology (*32*). For this purpose, a reaction coordinate was defined as the difference between the bond-making (C_E-N) and bond-breaking ($S-C_E$) distances. After equilibration and minimization of the system, we explored the potential energy surface, locating and characterizing a transition structure for the methyl transfer reaction. We then added a parabolic potential to the reaction coordinate at the corresponding value of the TS and ran molecular dynamic (MD) simulations. The procedure for the PMF calculation, which was traced down from the TS, was straightforward and required a series of MD simulations in which the reaction-coordinate variable was restrained around particular values. The different values of the variable sampled during the simulations were then pieced together to construct a distribution function from which the PMF was obtained. The value of the force constant used for the harmonic umbrella sampling (3000 kJ mol^{-1} $Å^{-2}$ on the reaction coordinate) was determined to allow a full overlapping of the different windows traced in the PMF evaluation. The length of each simulation window (15 ps of production after 5 ps of equilibration) and the total number of windows (80 in water and 120 in the enzyme) was proved to be long enough to sample the complete path of the reaction at a reference temperature of 300 K. During these constrained simulations, the variation of the reaction coordinate was saved in a file. These files were analyzed using the weighted histogram analysis method (WHAM) (*33*) to compute the PMF.

To obtain the respective PMF of the reaction in aqueous solution, we used a thermodynamic cycle. First, we obtained the PMF corresponding to two reacting fragments (glycine and SAM) where the relative orientation was restricted through the use of biasing potentials. In this way, the sampling of irrelevant structures is avoided. The relative orientation restrictions were unnecessary in the enzymatic PMF because the environment already imposes an adequate orientation of the fragments. The restricted PMF was then traced down from the TS until a flat region was reached. To get the full PMF in aqueous solution, we then estimated the free energy of releasing the restrictions imposed on our system, both in the reactant and the transition state, including that of the reaction coordinate in the former (*34*). For evaluating this term, we assumed a standard state 1M and that at large values, the reaction coordinate restriction may be treated as a distance restriction. We calculated the free energy associated with the release of the restraints for the transition state and the separated reactants and then added the difference (ΔG_{rel}) to the free energy barrier estimated from the restricted PMF ($\Delta G^{\ddagger}_{res}$) to obtain the true activation free energy ($\Delta G^{\ddagger}$) for the S_N2 displacement in water solutions. Details of the procedure can be found elsewhere (*35*, *36*). This strategy based on the restriction of the configurational space of the reactant fragments has been previously employed to obtain the PMFs corresponding to other bimolecular processes in solution (*35*, *37*) and for the calculation of binding free energies between flexible substrates and proteins (*38*).

Being aware that the AM1 method (used here for the QM region) does not always reproduce reaction barriers accurately enough, we considered a higher QM level correction (ΔE_{corr}), as the gas phase single-point energy barrier difference ΔE(MP2) − ΔE(AM1). MP2/6-31+G* and AM1 methods were employed for the QM subsystems, using averaged structures corresponding to the maximum and minimum of the free energy profiles; this was then added to the AM1/MM computed free-energy barrier for the total system. This simple correction scheme, based on the fact that the main source of error comes from the electronic description of the bond breaking/forming process in the semiempiricial Hamiltonian, has been successfully employed in several cases (*35*, *37*, *39*). Note that the calculated correction term is different in solution and in the enzyme because the transition and reactant state geometries are also different in both media. For these calculations SAM was modeled as a trimethylsulfonium ion.

Kinetic Isotope Effects Calculation. The rigid-rotor/harmonic-oscillator approximation was used with the CAMVIB/CAMISO programs (*40*, *41*) to calculate the intrinsic kinetic isotope effects (KIE) in solution and in the enzyme environment, with a semi classical correction of the tunnel effect computed by means of the Bell equation (*42*). QM/MM KIEs were thus calculated by using a subset comprising 59 atoms (equivalent to the QM regions). The TS structures used to compute the QM/MM KIEs were selected as the ones closest to the averages obtained in their respective windows of the PMF; these selected structures were subsequently fully

Scheme 1

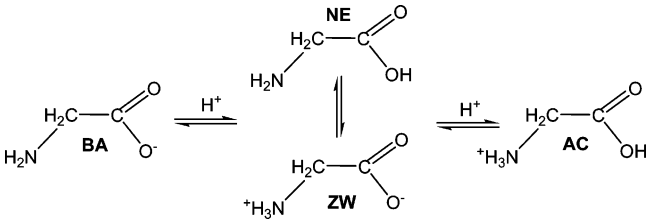

optimized to saddle points. The corresponding reactant structures were located from the IRC path traced down from the optimized saddle points. The Hessians computed for the QM atoms were subjected to a projection procedure to ensure that six zero frequencies were obtained for the translational and rotational modes and that the 3N-6 frequencies for the vibrational modes of the N quantum atoms satisfied the Teller−Redlich product rule (*43*).

RESULTS

Glycine Methylation in Aqueous Solution. In order to analyze the counterpart reaction of the enzymatic glycine methylation, we must first consider the different possible processes in which glycine can be involved in this medium. At neutral pH, the predominant form of glycine in aqueous solution is the zwitterionic tautomer (ZW), (*44*) formally obtained after an internal proton transfer from the carboxylic group to the amino group in the neutral tautomer (NE). The free energy difference between these two tautomers has been estimated to range between 7.3 and 7.7 kcal/mol at 298 K (*45*, *46*). This means that the ratio between the number of zwitterionic and neutral molecules is approximately $3 \cdot 10^5$. In addition to this tautomeric equilibrium, one should consider the acid/base equilibria leading to the basic form (BA, where glycine presents a deprotonated carboxylate group) and the acid form (AC, where the amino group is protonated). All these equilibria are shown in Scheme 1.

The p*K*a values of glycine are 2.34 and 9.6 at 298 K (*47*). This means that at pH 7, the ratio between molecules in the zwitterionic and basic forms is roughly 400, and the ratio between zwitterionic and acid forms is about $4.5 \cdot 10^4$. These ratios can be expressed as free energy differences (at 300 K) between ZW and BA of 3.6 kcal/mol and between ZW and AC of 6.4 kcal/mol, with the ZW form, in any case, being the most stable one.

Both the BA and NE forms are adequate candidates to go through methylation on the nitrogen atom. It must be taken into account that in this reaction, the transferring methyl group formally carries a positive charge, and thus, large electrostatic repulsions would be expected in the case of the ZW and the AC forms of glycine. Thus, we have analyzed two different possibilities corresponding to the reaction between SAM and BA and between SAM and NE. As explained in the Materials and Methods section, we have traced the corresponding AM1/TIP3P PMFs using the antysimmetric combination of the bond-making and bond-breaking distances as the distinguished reaction coordinate. As mentioned above, to avoid the sampling of irrelevant structures, the relative orientation of the reactive fragments (SAM and glycine) was restricted by means of the addition of biasing potential to selected internal angles and dihedrals. In particular, after some trials, we selected the SC_EN and C_ENC_α angles and the $C_ENC_\alpha C$ dihedral angle. In this way, the PMF can be easily traced down from the transition state to a flat region corresponding to the separated reactant fragments. The free energy barriers obtained in this manner are denoted as $\Delta G^{\ddagger}_{w,res}$. We then add the free energy difference associated with the release of the restraints in the transition and reactant states, ΔG_{rel}. The sum of both quantities gives the final AM1/MM estimation of the free energy barrier, $\Delta G^{\ddagger}_{w}(AM1)$. Finally, the correction term, ΔE_{corr}, was added to take into account the deficiencies associated with the semiempirical Hamiltonian. The final free energy barriers, $\Delta G^{\ddagger}$, and the different components are given in Table 1 for the methylation of the aqueous solution of the neutral (NE) and basic (BA) forms of glycine.

Table 1: Free Energy Barriers and Their Components (see Text) in kcal/mol for the Reaction between SAM and Glycine (Neutral and Basic Forms) in Aqueous Solution

medium	protonation state Gly	$\Delta G^{\ddagger}_{w,res}$ (AM1)	ΔG_{rel}	$\Delta G^{\ddagger}_{w}$ (AM1)	ΔE_{corr}	$\Delta G^{\ddagger}_{w}$
aqueous solution	NE	27.8	15.6	43.4	−16.0	27.4
	BA	23.9	15.8	39.7	−15.5	24.2

Table 2: Averaged Geometrical Parameters for the Transition States of Glycine Methylation in Aqueous Solution[a]

	$S-C_E$	C_E-N	$S-N$	$S-C_E-N$
NE glycine	2.22	2.04	4.25	172.4
BA glycine	2.20	2.05	4.23	170.9

[a] Distances in are Angstroms, and angles are in degrees.

For both possible substrates, the methylation reaction is described as a typical S_N2 process. In the TS, the methyl group is placed in between the donor and the acceptor atoms. Some key averaged geometrical parameters corresponding to the transition states are given in Table 2. The geometrical description of the two TSs is very similar, at least when comparing the relative positions of the donor, the acceptor, and the methyl group. The very slight diminution of the donor−acceptor (sulfur to nitrogen) distance could be due to the larger electrostatic interaction of the basic form of glycine with the positively charged methyl donor. This interaction is obviously shielded by the solvent, and the geometrical effect is very modest. The free energy barrier measured from the corresponding reactants for the methylation of the amino group of glycine by SAM is about 3.2 kcal/mol higher for the neutral than for the basic form. The S_N2 attack by the positively charged methyl group of SAM is favored in the basic form. Taking into account that at neutral pH the concentration of BA is about 10^3 times higher than the concentration of NE, we can conclude that the reaction in solution should take place through the basic form. Only in very acidic media (pH lower than 1) could the reaction rate for NE methylation be larger than that for BA.

Glycine Methylation Catalyzed by GNMT. The catalytic active site of GNMT contains several tyrosine and arginine residues involved in the binding of the cofactor and the substrate. In particular, Tyr33, Tyr220, Tyr194, and Arg175, in addition to Asn138 and Gly137, seem to establish close interactions with the substrate, whereas Arg40, Tyr21, and some other residues (Leu136, Ala64, Asn116, and Trp117) strongly interact with SAM (*21*). In order to assign the correct protonation state to each of these residues at the pH at which

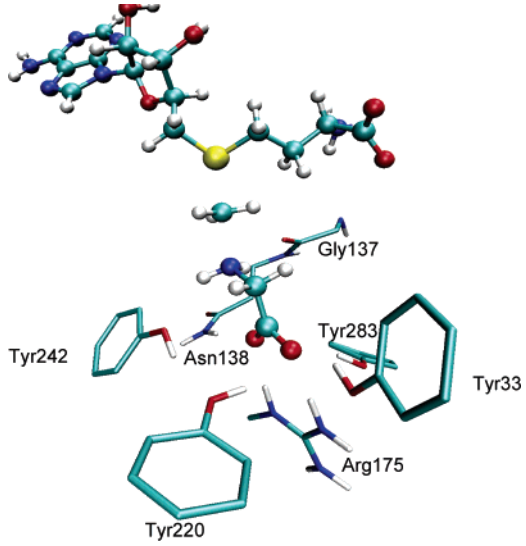

FIGURE 2: Snapshot of the GNMT active site in the transition state. SAM and glycine are shown in ball and stick representation. For the sake of clarity, only some key residues have been represented, and the nonpolar hydrogen atoms of the amino acids are not shown.

the experimental kinetic measurements were made (pH 7.2), we decided to recalculate the pK_a values using the cluster method, (*48*, *49*) as implemented by Field and co-workers, (*50*) according to which each titratable residue in the protein is perturbed by the electrostatic effect of the protein environment. This procedure has provided excellent results in other cases previously studied by some of us (*51*). We have carried out these calculations with and without the substrate in the active site, thus estimating the effect of the ionizable carboxylic group. We also considered the effect of the protein geometry using both the X-ray structure and a minimized one obtained after 400 ps of MD simulation. In all cases, the calculations indicate that tyrosine and arginine residues are in their protonated forms at pH 7.2, as otherwise expected. In fact, the pK_a values of arginines were found to be always larger than 14.0, and those of tyrosine were equal to or larger than 11.0. The pK_a calculations also revealed that the acid group of glycine is found in its deprotonated form in the enzyme active site. Considering that methylation requires a neutral amine group, we can conclude that the active form of the substrate for the enzymatic process is the basic one (BA). There is additional evidence of this finding in the fact that acetate acts as an inhibitor of the enzyme (*21*) and also in the fact that the maximum enzyme activity is found at basic pH (*52*). A question that remains unsolved is whether the enzyme just selects the BA form of the substrate from the solvent or whether it plays an active role in the transformation from ZW to BA, favoring the deprotonation of the ammonium moiety. It would be tempting to attribute this role to a deprotonated Arg175, which is placed very close to the glycine carboxylate group (Figure 2). However, our pK_a calculations show that this residue should be in its protonated state before the substrate enters into the active site. Another possibility could be that the change in the protonation state of the substrate takes place during the binding process. The glycine substrate is known to enter into the active site through the Tyr194 loop, which suffers important conformational changes after SAM binding (*21*). These changes could be related to an enzyme-mediated deprotonation of the substrate.

Table 3: Selected Averaged Distances (Å) and Angles (deg) in the Transition State and the Michaelis Complex of the Glycine Methylation Reaction in GNMT

	MC	TS
$S\cdots C_E$	1.82	2.24
$C_E\cdots N$	3.64	2.07
$S\cdots C_E\cdots N$	148.8	163.6
Arg175-$H_{NE}\cdots O_2$-Gly	4.72	3.11
Arg175-$H_{NH2}\cdots O_1$-Gly	2.24	2.56
Tyr33-$H_O\cdots O_2$-Gly	2.15	2.09
Tyr220-$H_O\cdots O_1$-Gly	2.75	3.18
Tyr220-$H_O\cdots O_2$-Gly	3.16	2.22
Tyr242-$O_H\cdots H_N$-Gly	2.95	2.35
Asn138-$H_N\cdots O_1$-Gly	1.96	2.03
Tyr283-$H_O\cdots O_2$-Gly	1.94	2.44
Gly137-$O\cdots H_N$-Gly	2.82	2.67

In any case, the active substrate form seems to be the BA form from which our reaction simulations were started.

The activation free energy for the enzymatic process at the AM1/MM level ($\Delta G_e^{\ddagger}(AM1)$) was obtained as the PMF difference between the maximum of the curve and the Michaelis complex, resulting in 28.8 kcal/mol. This is a common approximation because other contributions are usually small for these types of reactions (*36*, *53*). When this value is corrected considering the difference between the MP2/6-31+G* and the AM1 barriers, we obtained $\Delta G_e^{\ddagger}$ = 18.6 kcal/mol, very close to the value 18.2 kcal/mol, derived from the application of transition state theory (with a transmission coefficient equal to unity) to the experimental k_{cat} (*21*). This agreement gives us confidence in our computational approach, and therefore, we believe that it can be used to analyze enzymatic behavior and the origin of catalysis.

Figure 2 shows a representative structure of the transition state in GNMT. In this structure, the transferring methyl group is found in between the sulfur donor atom and the nitrogen atom of glycine. Averaged geometric parameters of the TS and the Michaelis complex are given in Table 3. We can observe that there is a network of hydrogen bonds established between the active site residues and glycine, both through the carboxylate group (O_1 and O_2 oxygens) and the amino group (with the polar hydrogen atoms). The hydrogen bond established with the amino group by means of Tyr242 and Gly137 are reinforced when passing from the Michaelis complex to the TS. This TS stabilization is surely a consequence of the positive charge that is being transferred with the methyl group. The resulting ammonium group can establish stronger hydrogen bond interactions. Interestingly, this strengthening of the hydrogen bonds with the amine group is not accompanied by a weakening of those hydrogen bonds established with the carboxylate group (Arg175, Tyr33, Tyr220, Tyr283, and Asn138). Although some hydrogen bonds are lengthened, others are shortened. During the advance of the reaction, glycine must reorientate in the active site in order to allow an optimum overlap of the nitrogen electron pair with the vacant orbital of the transferring methyl group. During this reorientation, the carboxylate group must break some interactions, but the process is assisted by the strengthening of other hydrogen bonds. This can be accomplished because of the network of hydrogen bond donor residues found in the active site. As we will show below, the final result of this delicate balance of hydrogen

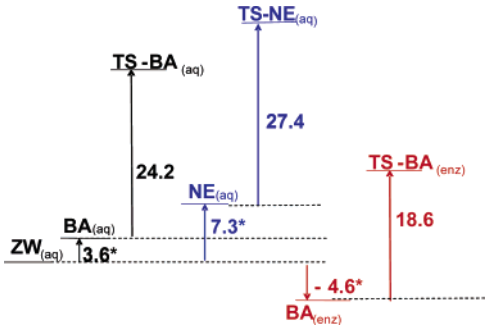

FIGURE 3: Free energy profiles for the SAM dependent methylation reaction of glycine in aqueous solution for the neutral form (in blue), the basic form (in black), and in the GNMT active site (red) at neutral pH. Energies are referred to solvated reactants, with the glycine in its most stable form (zwitterion). (*) indicates the values derived from experiments (see text).

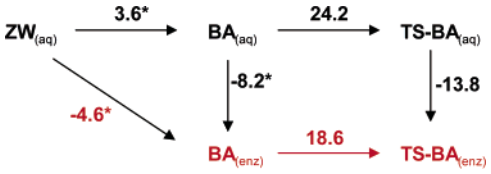

FIGURE 4: Schematic energy diagram for the SAM dependent methylation reaction of glycine to obtain the binding free energies of the reactant (BA) and the transition state (TS-BA) at neutral pH. Energies are reported in kcal·mol^{-1}. (*) indicates the values derived from experiments (see text).

bonds is a net stabilization of the transition state relative to the Michaelis complex.

Comparison between Enzymatic and In-Solution Processes: Origin of Catalysis in GNMT. A simple thermodynamic cycle shows that enzyme catalysis can be explained in terms of the larger affinity of the enzyme for the transition state than for the reactant state (*1*, *14*). However, this analysis can be deconstructed into more terms to emphasize, for example, the possible preferential stabilization of special reactant configurations (*13*). In the methylation of glycine, one must take into account the fact that the predominant protonation state of the substrate in aqueous solution and in the enzyme is different. Therefore, one could imagine a scenario where the reaction rate is increased by preferential stabilization of the basic form of glycine. In this section, we compare the binding free energies of the transition and reactant states, taking into account the change in the protonation state of the latter and also discuss the origin of the differences in these binding free energies.

As discussed before, most of the free glycine in solution is found in the zwitterionic form, and thus, it is the natural choice to establish a common origin among the different reaction paths presented here. In Figure 3, we present a comparison of the two reaction paths in solution (methylation on the NE and the BA forms) with the enzymatic process. The relative free energies of the NE and BA forms with respect to the prevalent ZW in aqueous solution can be derived from the experimental equilibrium constants of the tautomerization and protonation processes of glycine, assuming pH of 7.2. Regarding the enzymatic mechanism, we have obtained the binding free energy from the Michaelis constant as $\Delta G_{Bind} = RT \ln K_M$ (*21*). This binding energy is attributed to the $ZW_{(aq)} \rightarrow BA_{(enz)}$ process, considering that the Michaelis constant is derived from kinetic equations written as a function of the total free glycine concentration in solution and that the substrate is found in the basic form in the active site as discussed above.

We can now compare the different mechanisms considering a common origin. With respect to the glycine methylation in aqueous solution, the mechanism taking place through the basic form is clearly favored at neutral pH. The free energy barrier measured from the zwitterion form is 6.9 kcal/mol lower than for the methylation of the neutral form. This fact is because of the larger reactivity of the basic form, as shown before, but also of the larger concentration of BA in neutral aqueous solution that can be translated into a free energy difference between BA and NE of about 3.7 kcal/mol. Obviously, NE methylation in solution could be favored at acid pH because BA concentration would drop in those conditions.

The comparative analysis of BA methylation in solution and in the GNMT active site offers an opportunity to get a deeper insight into the origin of the catalytic efficiency of GNMT. From this energy diagram, the catalytic efficiency of GNMT can be estimated as a k_{cat}/k_{uncat} ratio of $5.6 \cdot 10^6$, corresponding to a reduction in the free energy barrier of 9.2 kcal/mol. The free energy profiles traced from the ZW form in aqueous solution allow us to establish the preference of the enzyme for the transition structure (Figure 4). Effectively, we can obtain the binding free energies corresponding to the transfer of the reactant (BA) or the transition state (TS-BA) from the solvent environment to the GNMT active site. The maximum free energy of binding, in absolute value, is attained at the transition state, $\Delta G_{Bind}(TS - BA) = -13.8$ kcal/mol. The origin of this binding energy is found in the strong hydrogen bond interactions established between the transition state and the enzyme. Of particular importance is the interaction between the negatively charged carboxylate of the substrate and the positively charged Arg175. Obviously, most of these interactions also play a decisive role, stabilizing the reactants in the basic form (BA). The binding free energy of the substrate in the reactant state is $\Delta G_{Bind}(BA) = -8.2$ kcal/mol, 5.6 kcal/mol lower than that for the transition state. An active site designed to fit the transition state can also display strong interactions with the reactant state if the charge distribution in the latter is similar enough to that of the former. This is the case in GNMT. However, there is also an additional effect stabilizing the transition state in the enzyme relative to the aqueous solution. As discussed above (Table 2), the transition state presents stronger hydrogen bonds for the glycine amine group, whereas carboxylate oxygen atoms do not suffer a significant desolvation.

There is another interesting point to take into account with respect to transition state stabilization. From the electrostatic point of view, the methylation reaction can be viewed as the transfer of a positive charge, carried by the transferring methyl group, from the S atom of SAM to the nitrogen atom of glycine. As shown in Scheme 2, this transfer implies an approach of the positive charge center to Arg175, a positively charged residue that plays an essential role in stabilizing the carboxylate group of glycine.

Then, it could be argued that the enzymatic environment could hinder the transfer process electrostatically. However, one must take into account that the reaction should be

Scheme 2

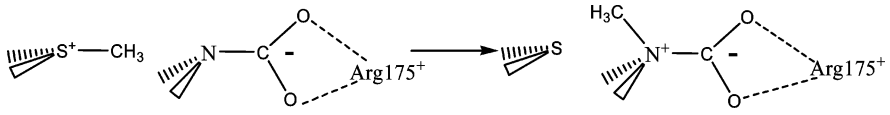

compared with the counterpart process in aqueous solution. In such a case, the reaction implies a decrease of the solute's dipole moment because the centroids of negative and positive charges become closer as the reaction advances. Thus, the reactant state is more stabilized in aqueous solution than the transition state, and the net solvent effect is an increase of the reaction barrier. To analyze this effect in solution and to compare it with the enzymatic environment, we have evaluated the averaged electrostatic potential experienced by a unit positive charge, located at positions along the vector connecting the donor S and the acceptor N atoms, because of the charge distribution of the MM environment both for the reaction in the GNMT active site and in aqueous solution. Figure 5 is a plot of the electrostatic potential created by the environment versus the fractional degree of methyl transfer (d_{SC}/d_{SN}), where 0 corresponds to the methyl group on the sulfur atom and 1 to the methyl group on the glycine nitrogen atom. The electrostatic potentials plotted in Figure 5 were computed using averaged structures for TS configurations in the enzyme and in solution. A negative value of the electrostatic potential indicates an attractive interaction between the +1 probe charge and the MM environment, whereas a positive value indicates a repulsive interaction. Clearly, the net effect of the electrostatic potential of the environment is a hindrance to the transfer of $CH_3^{\delta+}$ from S to N, both in water and in the enzyme active site. The potential is more positive on the N atom than on the S atom as is deduced from the position of both curves. The work required for methyl transfer, due to the environment, is the product of the partial positive charge and the electrostatic potential difference.

$$W = \delta q \times \Delta V$$

The arrows in Figure 5 indicate the position of the methyl group in the Michaelis complex, transition, and product states. The first conclusion from this analysis is that the potential on the methyl group is more negative in the enzyme, indicating a more favorable electrostatic interaction with the positively charged methyl group in this environment than that in water. Moreover, this picture shows that the increment in the electrostatic potential and, thus, the work needed to transfer the methyl group due to the effect of the MM environment is quite the same in solution and in the enzyme. That is, the enzyme does not hinder the transfer of a positive charge from SAM to glycine more than water, in spite of the presence of a positively charged residue close to the substrate.

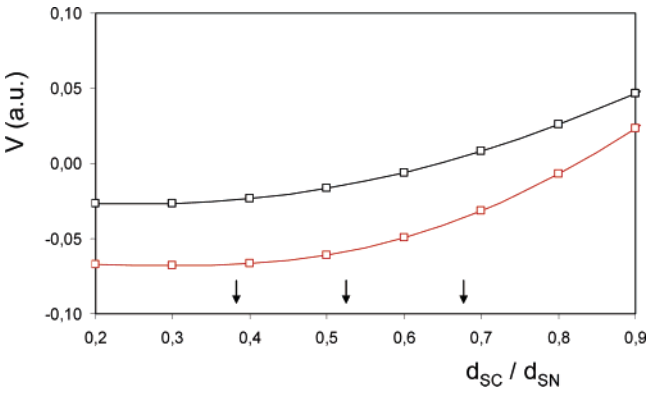

FIGURE 5: Plot of the electrostatic potential created by the MM environment vs the fractional degree of methyl transfer. The electrostatic potentials are computed using the averaged structures for TS configurations in the enzyme (red line) and in aqueous solution (black line). The arrows indicate the approximate position of the methyl group in the Michaelis complex, transition, and product states.

Considering the structural, energetic, and electrostatic analyses, we can conclude that the enzyme active site seems to be specifically designed to display favorable electrostatic interactions with the transition state. In the present case, most of these interactions (hydrogen bonds with the carboxylate and amine groups) also play an important role stabilizing the most reactive form of the substrate (the BA form), and thus, the binding free energies of the reactant and transition states are both quite large. However, and this is a key point, the enzymatic environment is able to stabilize the reactants in their more active BA forms without hindering the methyl transfer process. In energetic terms, the maximum binding energy (in absolute value) is obtained for the transition state.

Compression Hypothesis. The key proposal of the compression hypothesis, as formulated by Schowen (*54*), is that for enzymic methyl transfer reactions, mechanical compression by the enzyme might destabilize the reactants more than the TS, thus reducing the barrier for the catalyzed reaction compared with that for the uncatalyzed process in solution. In other words, if the TS for the S_N2 methyl transfer is more plastic than the reactant state for the catalyzed reaction, then mechanical compression by the protein might destabilize the reactants more than the TS. This compression hypothesis was introduced to explain the larger inverse secondary α-deuterium kinetic isotope effect (2° α-D KIE), $k/(CH_3)/k(CD_3)$, for methyl transfer catalyzed by catechol *O*-methyl transferase (COMT) with respect to the methylation of the methoxide ion by *S*-methyldibenzothiophenium ion in solution (*54*). This experimental finding was interpreted in terms of a tighter transition state with greater bond orders for the breaking and making of bonds in the enzymatic TS than those in the nonenzymatic one. The enzyme might be able to structurally distinguish the S_N2 TS from the preceding reactant state in order to specifically stabilize it (*55*). However, we recently showed that this compression hypothesis was not supported by AM1/MM calculations in the case of COMT (*43*). The computed Pauling bond orders (*56*) from the transferring methyl group to the nucleophile in each TS were significantly less than those to the leaving group, and also, the sum of the making and breaking bond orders was about the same for the enzyme and aqueous TSs. The main difference between COMT and GNMT methyl transfer reactions is that in the former, the methyl group is transferring to negatively charged oxygen atoms, whereas in the latter, the transfer takes place on a neutral amine group. It is thus

Table 4: Distances (Å) and Bond Orders Obtained for an Optimized Transition Structure in GNMT and in Aqueous Solution and the Primary C^{13} and Secondary α-D_3 KIEs Computed at 25 °C[a]

	bond order			bond length			average distance				
	S···C_E	C_E···N	S···N	S···C_E	C_E···N	S···N	S···C_E	C_E···N	S···N	C^{13}	α-D_3
water	0.28	0.12		2.24	2.13	4.34	2.20	2.05	4.23	1.059	0.786
enzyme	0.23	0.14		2.26	2.08	4.30	2.24	2.07	4.27	1.066	0.888

[a]The averaged values obtained from simulations of the transition states are also provided.

interesting to analyze this compression hypothesis for this different type of methyl transfer.

Table 4 shows the S−C_E, N−C_E, and S−N distances corresponding to an optimized representative transition structure in aqueous solution and in the enzyme, averaged distances, Pauling bond orders corresponding to the breaking and making of bonds, and primary C^{13} and secondary α-D_3 KIEs. These results do not support the compression hypothesis for GNMT. As in the case of COMT, the bond orders between the transferring methyl group and the nucleophile in each TS were significantly lower than those with the leaving group, and the sum of the making and breaking bond orders is slightly larger in aqueous solution than those in the enzyme TSs. In addition, although the donor−acceptor distance in the optimized structure is somewhat smaller in the enzyme than in water, the average distance obtained from MD simulations shows the opposite behavior: the distance now being slightly larger in the enzyme than in solution. These results, together with the computed 2° α-D_3 KIEs shown in Table 4 (C^{13} KIEs are almost equivalen,t but 2° α-D_3 KIEs are more inverse in solution than in the enzyme), show no computational evidence supporting the compression hypothesis. Nevertheless, as pointed out in our previous work (*43*), the terms tight and loose as applied to TSs can be ambiguous because a tight TS could also be one that is stiffer than a loose one, even with a similar geometry. The force constants for the out-of-plane bending angles (SCH and HCN angles) and the CH bond stretching of the transferring methyl group (which has been demonstrated to be responsible of the inverse KIE values) in the TS for the GNMT can be higher than the ones obtained in solution, thus describing a tighter TS. This possible ambiguity on the correlations between bond orders and force constants has to be kept in mind with regard to the interpretation of KIE measures.

CONCLUSIONS

Here we have presented the first QM/MM study on the reaction mechanism of Glycine *N*-methyltransferase. This enzyme catalyzes glycine methylation to yield sarcosine, a SAM dependent process that takes place through a S_N2 mechanism. The counterpart reaction in solution has been also studied in order to understand the origin of catalysis.

Because of tautomeric and protonation equilibria, glycine can be found in different forms in aqueous solution. At neutral pH, the dominant form is the zwitterion, which is not susceptible to N-methylation. The reaction can take place when the amine group is not protonated, such as in the basic and neutral forms. We have shown that at neutral pH, the reaction in solution proceeds through the basic form with a lower free energy barrier than through the neutral form. This is because of the fact that the concentration of the former in neutral solutions is larger than that for the latter and also because of the larger nucleophilic character of the amine group in the basic form.

The enzyme active site selectively stabilizes the basic form. The presence of a positively charged Arg175 favors the binding of a deprotonated carboxylate group. Although it could be argued that the presence of this positive group could hinder the methyl transfer from SAM to glycine, we have shown that this is not the case. The enzyme is able to stabilize the transition state of the reaction even more. A network of hydrogen bonds established with the amine and the carboxylate groups of glycine would explain that the binding energy reaches a maximum for the transition state.

A further insight into the origin of catalysis has been accomplished through the analysis of electrostatic effects. The electrostatic potential is better suited to interact with a transferring methyl group, which formally carries a positive charge, in the enzyme than in the solution. We finally tested whether the compression hypothesis supported this, in agreement with previous studies on other methyltransferases. The averaged donor−acceptor distance obtained from MD simulations is somewhat smaller in water than in the enzyme for the TS structure.

REFERENCES

1. Wolfenden, R., and Snider, M. J. (2001) The depth of chemical time and the power of enzymes as catalysts, *Acc. Chem. Res. 34*, 938−945.
2. Benkovic, S. J., and Hammes-Schiffer, S. (2003) A perspective on enzyme catalysis, *Science 301*, 1196−1202.
3. García-Viloca, M., Gao, J., Karplus, M., and Truhlar, D. G. (2004) How enzymes work: Analysis by modern rate theory and computer simulations, *Science 303*, 186−195.
4. Houk, K. N., Leach, A. G., Kim, S. P., and Zhang, X. Y. (2003) Binding affinities of host-guest, protein-ligand, and protein-transition-state complexes, *Angew. Chem., Int. Ed. 42*, 4872−4897.
5. Bruice, T. C., and Bruice, P. Y. (2005) Covalent intermediates and enzyme proficiency, *J. Am. Chem. Soc. 127*, 12478−12479.
6. Villa, J., and Warshel, A. (2001) Energetics and dynamics of enzymatic reactions, *J. Phys. Chem. B 105*, 7887−7907.
7. Warshel, A. (1998) Electrostatic origin of the catalytic power of enzymes and the role of preorganized active sites, *J. Biol. Chem. 273*, 27035−27038.
8. Warshel, A. (1978) Energetics of enzyme catalysis, *Proc. Natl. Acad. Sci. U.S.A. 75*, 5250−5254.
9. Page, M. I., and Jencks, W. P. (1971) Entropic contributions to rate accelerations in enzymic and intramolecular reactions and chelate effect, *Proc. Natl. Acad. Sci. U.S.A.* 68, 1678−1683.
10. Kollman, P. A., Kuhn, B., Donini, O., Perakyla, M., Stanton, R., and Bakowies, D. (2001) Elucidating the nature of enzyme catalysis utilizing a new twist on an old methodology: Quantum mechanical-free energy calculations on chemical reactions in enzymes and in aqueous solution, *Acc. Chem. Res. 34*, 72−79.
11. Mesecar, A. D., Stoddard, B. L., and Koshland, D. E. (1997) Orbital steering in the catalytic power of enzymes: Small structural changes with large catalytic consequences, *Science 277*, 202−206.
12. Menger, F. M. (1993) Enzyme reactivity from an organic perspective, *Acc. Chem. Res. 26*, 206−212.
13. Bruice, T. C. (2002) A view at the millennium: The efficiency of enzymatic catalysis, *Acc. Chem. Res. 35*, 139−148.

14. Martí, S., Roca, M., Andres, J., Moliner, V., Silla, E., Tuñón, I., and Bertrán, J. (2004) Theoretical insights in enzyme catalysis, *Chem. Soc. Rev. 33*, 98−107.
15. Kohen, A. (2003) Kinetic isotope effects as probes for hydrogen tunneling, coupled motion and dynamics contributions to enzyme catalysis, *Prog. React. Kinet. Mech. 28*, 119−156.
16. Fenimore, P. W., Frauenfelder, H., McMahon, B. H., and Young, R. D. (2004) Bulk-solvent and hydration-shell fluctuations, similar to alpha- and beta-fluctuations in glasses, control protein motions and functions, *Proc. Natl. Acad. Sci. U.S.A. 101*, 14408−14413.
17. Usdin, R., Borchardt, R. T., and Creveling, C. R. (1979) *Transmethylation*, Vol. 5, Elsevier-Nort-Holland, New York.
18. Blumenstein, J., and Williams, G. R. (1960) The enzymic N-methylation of glycine, *Biochem. Biophys. Res. Commun. 3*, 259−263.
19. Wittwer, A. J., and Wagner, C. (1981) Identification of the folate-binding proteins of rat-liver mitochondria as dimethylglycine dehydrogenase and sarcosine dehydrogenase - purification and folate-binding characteristics, *J. Biol. Chem. 256*, 4102−4108.
20. Kerr, S. J., and Heady, J. E. (1974) Modulation of tRNA methyltransferase activity by competing enzyme systems, *Adv. Enzyme Regul. 12*, 103−117.
21. Takata, Y., Huang, Y. F., Komoto, J., Yamada, T., Konishi, K., Ogawa, H., Gomi, T., Fujioka, M., and Takusagawa, F. (2003) Catalytic mechanism of glycine N-methyltransferase, *Biochemistry 42*, 8394−8402.
22. Konishi, K., and Fujioka, M. (1987) Chemical modification of a functional arginine residue of rat-liver glycine methyltransferase, *Biochemistry 26*, 8496−8502.
23. Velichkova, P., and Himo, F. (2005) Methyl transfer in glycine N-methyltransferase. A theoretical study, *J. Phys. Chem. B 109*, 8216−8219.
24. Field, M. J., Bash, P. A., and Karplus, M. (1990) A combined quantum-mechanical and molecular mechanical potential for molecular-dynamics simulations, *J. Comput. Chem. 11*, 700−733.
25. Singh, U. C., and Kollman, P. A. (1986) A combined ab initio quantum-mechanical and molecular mechanical method for carrying out simulations on complex molecular-systems: Applications to the Ch3cl + Cl− exchange-reaction and gas-phase protonation of polyethers, *J. Comput. Chem. 7*, 718−730.
26. Gao, J. L., and Xia, X. F. (1992) A priori evaluation of aqueous polarization effects through monte-carlo QM-MM simulations, *Science 258*, 631−635.
27. Gao, J. L., and Truhlar, D. G. (2002) Quantum mechanical methods for enzyme kinetics, *Annu. Rev. Phys. Chem. 53*, 467−505.
28. Field, M. J., Albe, M., Bret, C., Proust-De Martin, F., and Thomas, A. (2000) The dynamo library for molecular simulations using hybrid quantum mechanical and molecular mechanical potentials, *J. Comput. Chem. 21*, 1088−1100.
29. Dewar, M. J. S., Zoebisch, E. G., Healy, E. F., and Stewart, J. J. P. (1985) The development and use of quantum-mechanical molecular-models. 76. Am1: A new general-purpose quantum-mechanical molecular-model, *J. Am. Chem. Soc. 107*, 3902−3909.
30. Damm, W., Frontera, A., TiradoRives, J., and Jorgensen, W. L. (1997) OPLS all-atom force field for carbohydrates, *J. Comput. Chem. 18*, 1955−1970.
31. Jorgensen, W. L., Chandrasekhar, J., Madura, J. D., Impey, R. W., and Klein, M. L. (1983) Comparison of simple potential functions for simulating liquid water, *J. Chem. Phys. 79*, 926−935.
32. Torrie, G. M., and Valleau, J. P. (1977) Non-physical sampling distributions in Monte-Carlo free-energy estimation: Umbrella sampling, *J. Comput. Phys. 23*, 187−199.
33. Kumar, S., Bouzida, D., Swendsen, R. H., Kollman, P. A., and Rosenberg, J. M. (1992) The weighted histogram analysis method for free-energy calculations on biomolecules. 1. The method, *J. Comput. Chem. 13*, 1011−1021.
34. Hermans, J., and Wang, L. (1997) Inclusion of loss of translational and rotational freedom in theoretical estimates of free energies of binding. Application to a complex of benzene and mutant T4 lysozyme, *J. Am. Chem. Soc. 119*, 2707−2714.
35. Roca, M., Martí, S., Andrés, J., Moliner, V., Tuñón, M., Bertrán, J., and Williams, A. H. (2003) Theoretical modeling of enzyme catalytic power: Analysis of "cratic" and electrostatic factors in catechol O-methyltransferase, *J. Am. Chem. Soc. 125*, 7726−7737.
36. Roca, M., Moliner, V., Ruiz-Pernía, J. J., Silla, E., and Tuñón, I. (2006) Activation free energy of catechol O-methyltransferase. Corrections to the potential of mean force, *J. Phys. Chem. A 110*, 503−509.
37. Soriano, A., Silla, E., Tuñón, I., Martí, S., Moliner, V., and Bertrán, J. (2004) Electrostatic effects in enzyme catalysis: a quantum mechanics/molecular mechanics study of the nucleophilic substitution reaction in haloalkane dehalogenase, *Theor. Chem. Acc. 112*, 327−334.
38. Woo, H. J., and Roux, B. (2005) Calculation of absolute protein-ligand binding free energy from computer simulations, *P. Natl. Acad. Sci. U.S.A. 102*, 6825−6830.
39. Martí, S., Andres, J., Moliner, V., Silla, E., Tuñón, I., Bertrán, J., and Field, M. J. (2001) A hybrid potential reaction path and free energy study of the chorismate mutase reaction, *J. Am. Chem. Soc. 123*, 1709−1712.
40. Williams, I. H. (1982) On the representation of force-fields for chemically reacting systems, *Chem. Phys. Lett. 88*, 462−466.
41. Williams, I. H. (1983) Force-constant computations in Cartesian coordinates: Elimination of translational and rotational contributions, *Theochem. 11*, 275−284.
42. Bell, R. P. (1980) *The Tunnel Effect in Chemistry*, Chapman and Hall, London.
43. Ruggiero, G. D., Williams, I. H., Roca, M., Moliner, V., and Tuñón, I. (2004) QM/MM determination of kinetic isotope effects for COMT-catalyzed methyl transfer does not support compression hypothesis, *J. Am. Chem. Soc. 126*, 8634−8635.
44. Tortonda, F. R., Pascual-Ahuir, J. L., Silla, E., and Tuñón, I. (1996) Why is glycine a zwitterion in aqueous solution? A theoretical study of solvent stabilising factors, *Chem. Phys. Lett. 260*, 21−26.
45. Haberfield, P. (1980) What is the energy difference between $H_2NCH_2CO_2H$ and $^+H_3NCH_2CO_2^-$, *J. Chem. Educ. 57*, 346−347.
46. Wada, G., Tamura, E., Okina, M., and Nakamura, M. (1982) On the ratio of zwitterion form to uncharged form of glycine at equilibrium in various aqueous-media, *Bull. Chem. Soc. Jpn. 55*, 3064−3067.
47. Lide, D. R. E. (1996) *Handbook of Chemistry and Physics*, 77th ed., p 7−1, CRC Press, Boca Raton, FL.
48. Gilson, M. K. (1993) Multiple-site titration and molecular modeling - 2 rapid methods for computing energies and forces for ionizable groups in proteins, *Proteins 15*, 266−282.
49. Antosiewicz, J., Mccammon, J. A., and Gilson, M. K. (1994) Prediction of Ph-dependent properties of proteins, *J. Mol. Biol. 238*, 415−436.
50. Field, M. J., David, L., and Rinaldo, D., personnal communication.
51. Ferrer, S., Silla, E., Tuñón, I., Oliva, M., Moliner, V., and Williams, I. H. (2005) Dependence of enzyme reaction mechanism on protonation state of titratable residues and QM level description: lactate dehydrogenase, *Chem. Commun.*, 5873−5875.
52. Ogawa, H., and Fujioka, M. (1982) Purification and properties of glycine N-methyltransferase from rat-liver, *J. Biol. Chem. 257*, 3447−3452.
53. Schenter, G. K., Garrett, B. C., and Truhlar, D. G. (2003) Generalized transition state theory in terms of the potential of mean force, *J. Chem. Phys. 119*, 5828−5833.
54. Hegazi, M. F., Borchardt, R. T., and Schowen, R. L. (1979) Alpha-deuterium and C-13 isotope effects for methyl transfer catalyzed by catechol O-methyltransferase: Sn2-like transition-state, *J. Am. Chem. Soc. 101*, 4359−4365.
55. Olsen, J., Wu, Y. S., Borchardt, R. T., and Schowen, R. L. (1979) *Transmethylation*, Elsevier, New York.
56. Bond order $n = \exp[(R1 - Rn)/c]$, where $c = 0.6$.

BI061319K